JOC The Journal of Organic Chemistry

Article

Synthesis of 5,12-Diazapentacenes and Their Properties

Rosalva C. Garcia, Matthew J. Pech, Roger D. Sommer, and Christopher B Gorman

J. Org. Chem., **Just Accepted Manuscript** • DOI: 10.1021/acs.joc.9b01628 • Publication Date (Web): 04 Nov 2019

Just Accepted

is published by the American Chemical Society. 1155 Sixteenth Street N.W., Washington, DC 20036

Synthesis of 5,12-Diazapentacenes and Their Properties

Rosalva C. Garcia, Matthew J. Pech, Roger Sommer, and Christopher B. Gorman*

Department of Chemistry, North Carolina State University, Box 8204, Raleigh, NC 27695, USA

Diazapentacenes, N-heteroacenes, organic electronics

ABSTRACT: An efficient synthesis via a precursor route to a new class of linear dialkyldiaminoazapentacenes is reported. The synthetic route involves the coupling of 4-substituted aniline derivatives to 2,5-dibromoterephthalonitrile via Buchwald-Hartwig amination followed by an acid-mediated cyclization to furnish the diazapentacenes. These reactions occur under short reaction times (<2 h.) and high yields (77–99%) and do not require column chromatography for purification. The electrochemical and optical properties of the diazapentacenes were evaluated, and the values indicate that these molecules are promising n-type materials for organic electronic devices. The photostability of these molecules was significantly greater than unsubstituted acenes. Their method of degradation via endoperoxide generation was confirmed by X-ray crystallography and mass spectrometry.

INTRODUCTION

The market for flexible electronics is expected to reach 70 billion USD by 2026.[1] One strategy to achieve the properties of flexibility, light-weight, and low-cost in electronics is to incorporate organic-based materials as the key components in the electronic devices as organic field-effect transistors (OFETs), organic light-emitting diodes (OLEDs), organic photovoltaics (OPVs), organic resistive memories (ORMs), and organic sensors. Specifically, there is interest in the development of complementary organic circuits based on p- and n-type materials for hole and electron charge carriers in OFETs in the next generation of organic electronics.[2] Currently, there is a shortage of n-type materials compared to their counter p-type due to issues arising from ambient stability, charge carrier mobility, and energy alignment.[3–6]

Acenes, molecules with linearly fused benzene rings, have been used in electronics as the organic material in organic thin-film transistors (OTFTs), OFETs, and OLEDs.[7,8] Diazapentacenes, also known as N-heteroacenes, are analogs of acenes in which a CH moiety is substituted with an imino-nitrogen atom where the number and position of the nitrogen atoms in the backbone can affect the electronic structure, molecular packing, solubility, and stability.[9–13] Because the imino-nitrogen atoms stabilize the N-heteroacene by lowering its LUMO level, N-heteroacenes are promising candidates for organic n-type semiconductors.[14] Thus, there is interest in the development of novel N-heteroacenes and their properties.

Traditionally, N-heteroacenes have been prepared by condensation reactions. However, these reactions between aromatic *o*-diamines with aromatic *o*-dihydroxy compounds yielded N-heteroacenes but functional group tolerance was low due to the harsh conditions that can result in the decomposition of the starting materials.[15] Recently, there was a report of a 12,14-disubstituted 5,7-diazapentacenes via a Friedländer condensation followed by an oxidation; however, the yields were moderate to poor.[16] In addition to the moderate to poor yields, the authors report difficulties to synthesize the initial precursors, to dehydrogenate the alternative precursors to the fully aromatized 5,7-diazapentacenes, and to crystallize their one 5,7-diazapentacene molecule.[16] Furthermore, the synthesis of larger N-heteroacenes, such as N-heteropentacene and N-heterohexaacene, resulted in the N,N'-dihydro compounds due to the increased difficulty of oxidizing them. A more recent approach in the synthesis of larger, substituted N-heteroacenes used palladium-catalyzed coupling. In the synthesis of alkynylated N-heteropentacenes, this method works the best with activated halides, and it has limitations with deactivated halides.[17] These limitations make new approaches for the synthesis of N-heteroacenes of interest.

Here, we present a synthetic route for 5,12 diazapentacenes with C_{2h} symmetry in high yields with short reaction times. The route involves the synthesis of a diazapentacene precursor followed by an acid-mediated cyclization to obtain the diazapentacene. A similar coupling and cyclization was performed on a dihexyl ketone using copper in one pot, albeit a low yield, for the synthesis of 5,7-diazapentacene derivatives which degrade by forming the dimer structure.[18] In this work, the outstanding feature of the syntheses of the building block, precursors, and diazapentacenes is the ease of synthesis, high yields, and no need of column chromatography for purification.

RESULTS AND DISCUSSION

Synthesis of Diazapentacenes. First, 2,5-dibromoterephthalonitrile (**1**), a building block for the diazapentacene precursors, was synthesized (Scheme 1). The synthesis of this molecule has been reported[19] and it was optimized to reduce the overall reaction time

to 4 h and to increase the overall yield to 83%. Key to the optimization involved adding the acyl chloride to the ammonium hydroxide as opposed to the reversed addition which reduced the amidation step from a 3-hour reaction to a 5-minute reaction and increased the yield from 76% to 94%. The electron withdrawing nitrile groups were placed on the aryl halide to facilitate the oxidative addition step in the Buchwald-Hartwig catalytic cycle.[20]

Scheme 1. Synthesis of 2,5-dibromoterephthonitrile (1). Conditions: i.) $(COCl)_2$, cat. DMF, DCM, reflux, 3 h.; ii). NH_4OH, RT, 5 min.; and iii) $POCl_3$, 110 °C, 1 h.

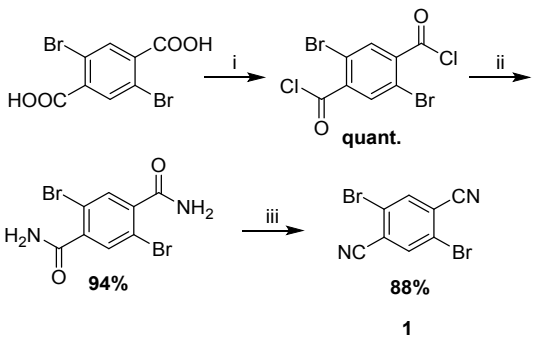

The diazapentacenes were synthesized via a precursor route (Scheme 2). The precursors were synthesized by the Buchwald-Hartwig amination of **1** and commercially available 4-substituted anilines. For this coupling, it was important to use the palladium precursor Brettphos Pd G1 to take advantage of its high selectivity for monoarylation.[21] The identity of these compounds was confirmed by ^{1}H and ^{13}C NMR spectroscopy as well as single crystal X-ray crystallography (Figure S26-S28). The diazapentacenes were obtained from an acid-mediated cyclization of the precursors with trifluoroacetic acid (TFA) and/or trifluoromethanesulfonic acid (TFMSA) using a previous report for the synthesis of 9-aminoacridine (**9-AA**).[22] It is noteworthy that the syntheses of the precursors and diazapentacenes proceed in relatively short reaction times with high yields and do not require column chromatography for purification.

Scheme 2. Synthesis of diazapentacenes via a precursor route. Conditions: i.) BrettPhos Pd G1, Cs_2CO_3, *t*-BuOH, 80 °C, 2 h. and ii.) TFA and/or TFMSA, 60 °C, 1 h.

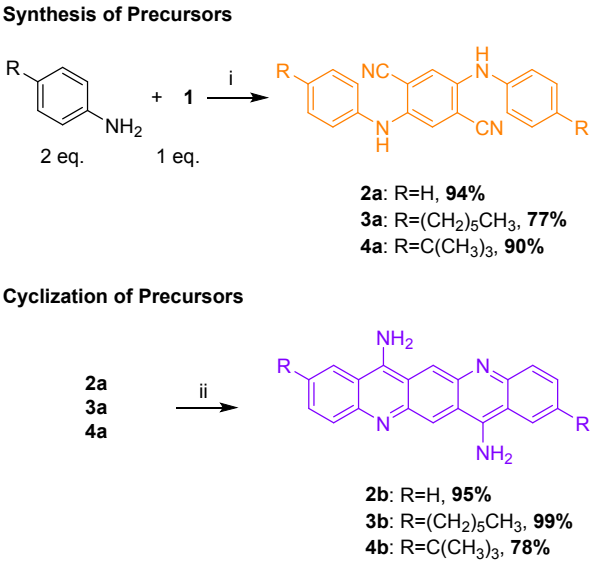

The placement of the nitrile groups on the center ring of the diazapentacene precursor has two purposes. First, placement here should favor the second cyclization in an acidic environment by making the carbon of the nitrile group more electrophilic. Under the strongly acidic conditions employed, the pyridyl and aniline nitrogens are protonated (Scheme 3a). If the nitrile groups were placed on the outer benzene rings, then the pyridinium ion would reduce the nucleophilicity of the carbon on the adjacent benzene ring which can be detrimental to the second cyclization (Scheme 3b). Second, as long as the aniline building block has a line of symmetry through the amino group, then it is anticipated that the cyclization of the precursor will yield the linear diazapentacene when the nitrile groups are on the center benzene ring. Otherwise, when the nitrile groups are situated on the outer benzene rings, then there are two potential products, the bent and the linear structure. Of these two products, there is a preference for the bent structure as it is more stable than the linear structure in accordance with Clar's rule.[23] This phenomenon has been reported in the literature.[24] Indeed, it is observed that the cyclization of the precursor shown in Scheme 3b results in the recovery of starting material at 60 °C and a mixture of products at higher temperatures.

Scheme 3. General schematic for the electronics of the second cyclization in an acidic environment and the diazapentacene structures for precursors with (a) the nitrile group on the center and with (b) nitrile groups on the outer benzene rings.

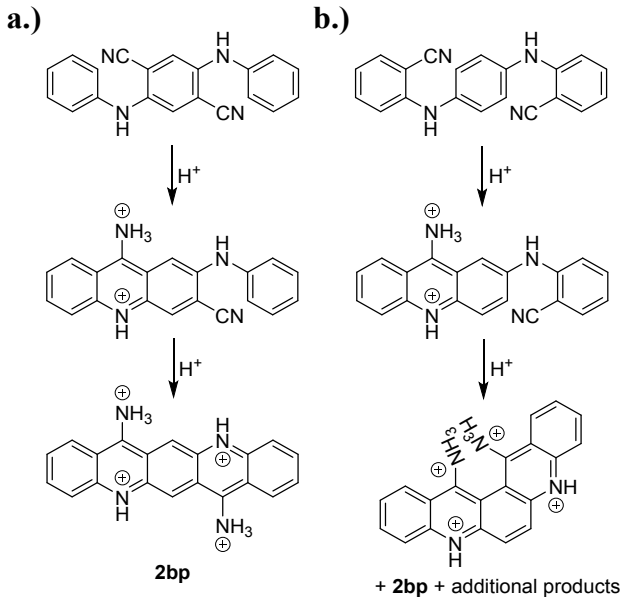

Optical, Electrical, and Photophysical Properties. It has been reported that, in acenes, there is a bathochromic shift of the longest wavelength absorption by approximately 100 nm with each benzannulation.[25] The UV-visible absorption spectra of **2b**, **3b**, and **4b** were obtained and compared to **9-AA**, the three-ring analogue (Figure 1a). Indeed, there is approximately an increase of ~200 nm from **9-AA** with λ_{max} = 424 nm to **2b**, **3b**, and **4b** with λ_{max} = 648 nm, 649 nm, and 638 nm, respectively. Furthermore, the UV-visible absorption spectra were used to calculate the optical HOMO-LUMO gaps (E_g) to 1.86 eV, 1.82 eV, and 1.83 eV for **2b**, **3b**, and **4b**, respectively, using their λ_{onset} = 668 nm, 680 nm, and 679 nm, respectively. These E_g values are also consistent with the trend where E_g=1/n where n is the number of rings.

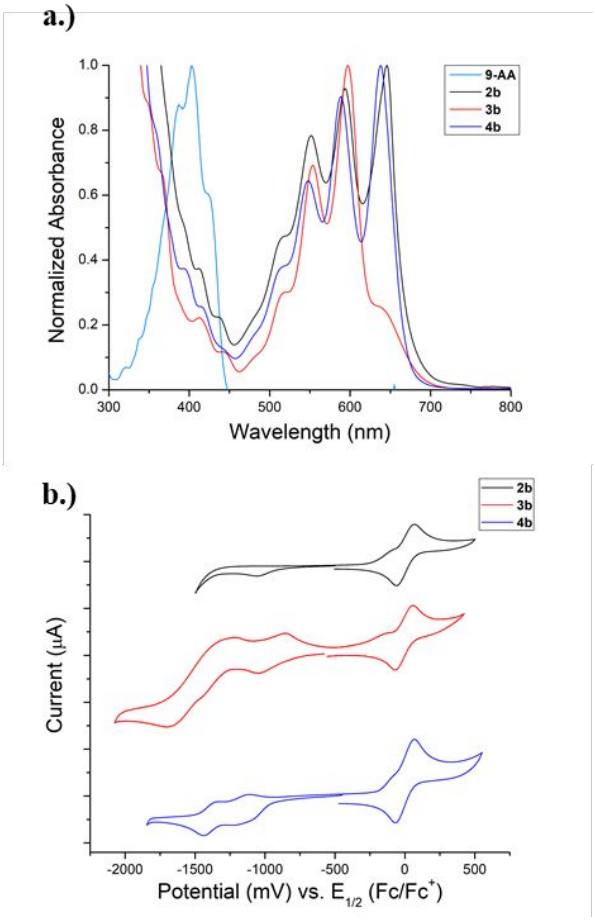

Figure 1. (a) UV-Visible absorption spectra of **9-AA**, **2b**, **3b**, and **4b** in 50:50 THF:MeOH and (b) the cyclic voltammograms of **2b**, **3b**, and **4b** in 0.1 M *n*-Bu_4PF_6 in THF at 50 mV/s.

Cyclic voltammetry measurements of **2b**, **3b**, and **4b** were carried out in THF using ferrocene as an internal standard (Figure 1b). Diazapentacene **2b** has one irreversible reduction peak whereas diazapentacenes **3b** and **4b** have two reversible redox peaks. Based on these reduction potentials, the LUMO energy levels for **2b**, **3b**, and **4b** where calculated to -3.88 eV, -3.97 eV, and -3.78 eV vs. Fc/Fc^+, respectively. These LUMO energy levels are not below the threshold reported of -4.1 eV for n-type materials stable in air.[26] However, these LUMO energy levels are close to or within range of -3.9 eV to -4.1 eV in which electron transport can be obfuscated by the degradation of molecules by oxygen and/or water.[5,26] Nonetheless, electron transport may be viable if the material is protected from air. Since oxidations were not observed for these molecules, the HOMO energy levels were calculated to -5.74 eV, -5.79 eV, and -5.61 eV using the onset wavelength for λ_{max} (Table 1).

Table 1. Summary of the optical and electrical properties of 2b, 3b, and 4b in THF.

Compound	Optical		Electrical		
	λ_{max} (nm)	E_g, opt. (eV)[a]	$E_{red.}$ (V)	LUMO[b]	HOMO[c]
2b	648	1.86	-0.92	-3.88	-5.74
3b	649	1.82	-0.83	-3.97	-5.79
4b	638	1.83	-1.02	-3.78	-5.61

[a] E_g, opt. (eV) =1240/ λ_{onset} (nm).

[b] Calculated as following: $E_{LUMO} = -4.80 - E_{red.}$

[c] Calculated as following: $E_{HOMO} = E_{LUMO} - E_g$, opt.

Emission spectra were collected in MeOH since the peaks in absorption spectra of the dry diazapentacene in THF were not well defined without the slight addition of water (Figure S16). This poor peak resolution was not observed in dry methanol. Furthermore, because these diazapentacenes contain a 4-aminopyridine moiety, then various reactions such as excited state proton transfer may

occur. When the neutral molecule **2b** was excited at 450 nm, negative Stokes shifts were observed (Figure 2a). This may be due to emission from $S_n \rightarrow S_0$ where n>1. It is also possible that excited state proton transfer, can occur.[27] However, the emission spectrum of the fully protonated species of **2b** (**2bp**) (*vida infra*) has a positive Stokes shift of 17 nm (Figure 2b), suggesting that additional photophysical complexities are eliminated in these species. Furthermore, a single exponential decay time constant of 13.6 ns was found for **2bp**. The absorption and emission spectra of **3b**, **3bp**, **4b**, and **4bp** are shown in the SI (Figure S17 and Figure S18). The time constants for **3bp** and **4bp** are 10.1 ns and 10.6 ns, respectively.

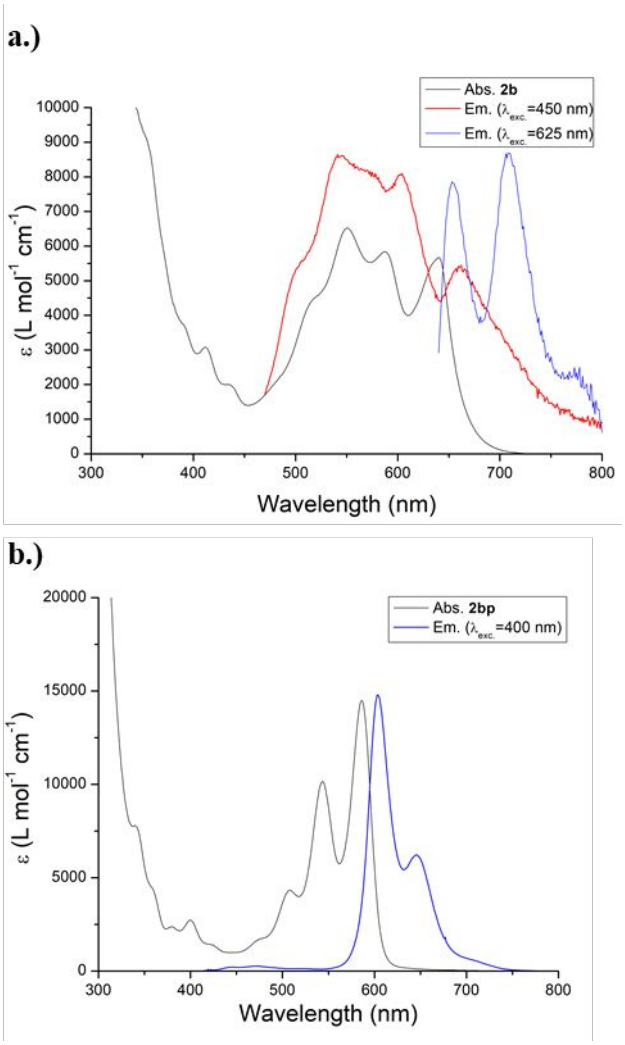

Figure 2. UV-Visible absorption and emission spectra of (a) **2b** and (b) **2bp**.

Like **2bp**, **3bp** and **4bp** also have small Stokes shift, 20 and 25 nm, respectively. A small Stokes shift is reflective of the rigid molecular geometry of the diazapentacenes.[28,29] Furthermore, small Stokes shifts are promising for exhibiting a low reorganization energy in charge transport. In addition to obtaining a Stokes shift, quantum yields (Φ) of the protonated diazapentacenes were obtained and calculated to 0.38, 0.30, and 0.29. The Stokes shift and quantum yields are summarized in Table 2.

Table 2. Photophysical properties for 2bp, 3bp, and 4bp in MeOH.

Compound	Stokes shift (nm)	Φ	τ (ns)
2bp	17	0.38	13.6
3bp	20	0.30	10.1
4bp	25	0.29	10.6

Acidochromism. The diazapentacenes **2b**, **3b**, and **4b** possess four nitrogen atoms that could be protonated, and thus these molecules are expected to exhibit acidochromism upon the addition of up to four equivalents of acid. Because there are two different types of nitrogen atoms, it was hypothesized the first two equivalents of acid would protonate the pyridyl nitrogen atoms since their lone pairs

are orthogonal to the π-system. Then, the addition of two more equivalents of acid should protonate the amino nitrogen atoms. This order of protonation has been reported in 9-aminoacridine and 4-aminopyridine.[30,31]

The absorption spectra for **2b** do not change significantly with the addition of the first two equivalents of TFA (Figure 3a) which is congruent with the protonation of the pyridyl nitrogen atoms. The addition of two more equivalents of TFA to **2b** (Figure 3b) results in hypsochromic shifts for the longest wavelength from λ_{max} = ~640 nm to λ_{max} = ~600 nm. This trend is consistent with the protonation of the amino nitrogen atoms whose lone pairs are no longer in resonance with the π-system, decreasing the number of conjugated atoms. The addition of TFA after roughly four equivalents of TFA does not change the spectrum, as expected, since there are no more sites for protonation. Molecules **3b** and **4b** exhibit the same behavior (Figure S19 and S20). This acidochromic behavior of the diazapentacenes makes them candidates for metal ion- and proton-sensing applications.[14]

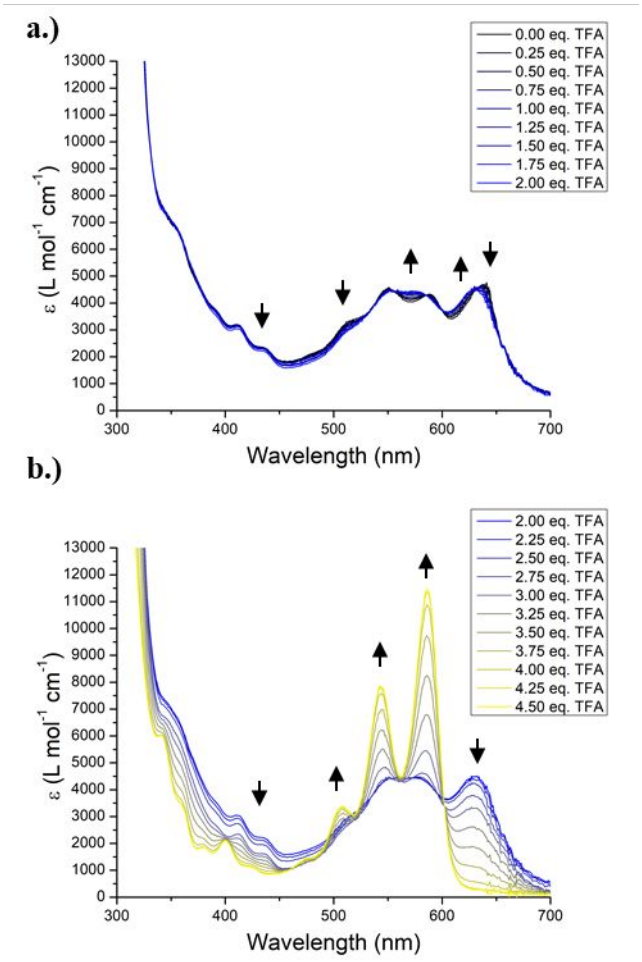

Figure 3. Acidochromism of **2b** (a) upon the addition of 0.0-2.0 equivalents of TFA and (b) upon 2.0-4.5 equivalents of TFA in methanol.

Stability. With increasing molecular length, acenes are known to degrade by dimerizing or oxidizing via Diels-Alder reactions. To evaluate the photooxidative stability of acenes and N-heteroacenes, some researchers choose to monitor the decrease of absorbance over time in air-free solutions and UV light while others choose ambient air and light.[32–35] In this

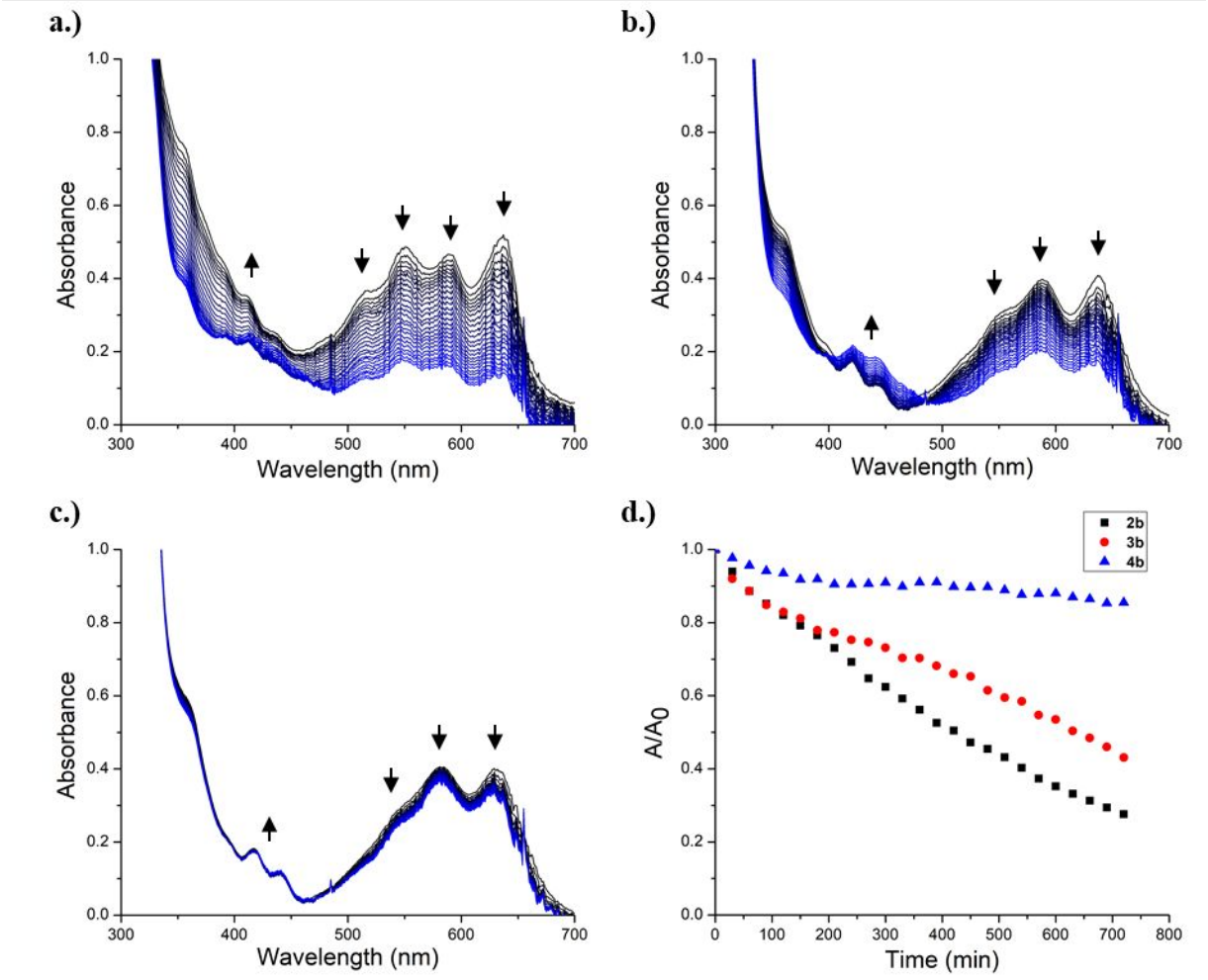

Figure 4. Photodegradation studies of (a) **2b**, (b) **3b**, and (c) **4b**. (d) Plot of A/A_0 vs time for **2b**, **3b**, and **4b**.

work, the degradation studies were carried out under ambient air and light. To validate these conditions, the degradation of pentacene, as a reference, was studied and its half-life was calculated to 11.0 min. when monitoring the absorbance (A) of λ_{max} = 575 nm over the initial absorbance (A_0) (Figure S21). While the kinetics for the degradation of these molecules may be complicated, many researchers report degradation data with plots of A/A_0 versus time. The half-life of pentacene in THF under air-saturated and ambient light has been reported to be 10±3 min.[36] Based on results for the degradation of pentacene in THF, the degradation of the diazapentacenes were carried out under ambient air and light over a period of 12 h (Figure 4a, b, and c). A plot of A/A_0 for **2b**, **3b**, and **4b** at λ_{max} = 637 nm, 637 nm, and 629 nm, respectively, (Figure 4d) shows "half-lives" of 420 min. and 630 min. for **2b** and **3b**. For **4b**, after 12 h, the A/A_0 was 0.86. These degradation studies illustrate an enhanced stability of the diazapentacenes **2b**-**4b** compared to other N-heteropentacenes in the literature.[9]

While pentacene can degrade via dimerization or oxidation, it is highly susceptible to degradation via the endoperoxide formation to form the quinone via a Diels-Alder reaction with molecular oxygen.[37] The mass spectrum of the residual pentacene from the photodegraded sample was analyzed for the dimer ($C_{44}H_{28}$) and endoperoxide ($C_{22}H_{14}O_2$). The endoperoxide with a proton adduct was found with an experimental mass of 311.1067 which is within 1.3 ppm of the theoretical mass of 311.1072. Likewise, the byproducts of the photodegradation of the diazapentacenes were studied by mass spectrometry. Diazapentacene **2b**-**4b** showed the corresponding mass for the quinone product (Figure S22) where the quinone was not observed in the HRMS of the diazapentacenes (Figures S23-S25). The formation of the quinone structure can also be confirmed by the crystal structures of the oxidized diazapentacenes.

Crystallizations of the diazapentacenes were attempted via solvent evaporation of the samples in DMSO in NMR tubes where the solutions were kept in the dark to minimize the degradation of the diazapentacenes. From these crystallizations, purple crystals, as opposed to the orange color for the precursors, were obtained. However, when the crystallographic data was received, the structures obtained were for the oxidized diazapentacenes **2b** and **3b** (Figures S29 and S30). From these crystal structures, it can be surmised that the targeted diazapentacenes were synthesized. Degradation of pentacene to the endoperoxide and the quinone has been reported in the literature.[37]

CONCLUSIONS

This article reported a two-step synthetic method for the synthesis of 5,12 diazapentacenes via a precursor route with excellent yields (>77%) and short reaction times (<2 h.). The purification is relatively simple and does not require column chromatography. The ease of synthesis and purification enables the synthesis of novel diazapentacene derivatives for the analysis of structure-property relationships.

The characterization of the diazapentacenes in this work reveal their potential as reasonable candidates in organic electronics. The optical data show the diazapentacenes **2b**, **3b**, and **4b** have optical HOMO-LUMO gaps of 1.86, 1.82, and 1.83 eV which are consistent with other five-ringed azaacenes. While these 5,12 diazapentacenes undergo photooxidation as confirmed by X-ray crystallography and mass spectrometry, they are more stable than other N-heteroacenes as shown by **4b** which as A/A_0 = 0.86 after 12 h. From cyclic voltammetry, the LUMO energy levels are -3.88 eV, -3.97 eV, and -3.78 eV vs. Fc/Fc^+ which can be acceptable materials for electron transport. Lastly, these diazapentacenes exhibit acidochromism up to four equivalents of acid. The fully protonated diazapentacenes have small Stokes shifts ranging from 17 to 25 nm which is characteristic of a rigid structure that is promising for electron transport in thin film devices.

Overall, this synthetic route gives access to the synthesis of diazapentacenes with a unique distribution of the imino-nitrogen atoms in the framework of the acene for research on structure-property relationships. These molecules are relatively easy to synthesize in high yields and appear to have increased ambient stability compared to other diazapentacenes.

EXPERIMENTAL SECTION

Materials.

All reagents were purchased from commercial sources and used without further purification unless otherwise specified. The palladium precursor catalyst BrettPhos Pd G1 was purchased from Sigma-Aldrich. Dichloromethane (DCM) and tetrahydrofuran (THF) were obtained from a solvent purification system. Dimethylformamide (DMF) and *t*-butanol (*t*-BuOH) were distilled and stored over 4 Å molecular sieves. Thin-layer chromatography (TLC) was performed on Biotage's KP-SIL TLC plates and visualized under UV light.

Instrumentation.

Nuclear magnetic resonance spectra were recorded at room temperature on a Varian Inova 400 MHz NMR spectrometer or on either a Bruker Avance NEO 700 MHz or Bruker Avance III 700 MHz NMR spectrometer. The chemical shifts (δ) are reported in ppm and the abbreviations used to describe the multiplicities are as following: s (singlet), d (doublet), t (triplet), and m (multiplet). FT-IR spectra were recorded on a Bruker Platinum-ATR spectrometer. Melting points were determined using a MEL-TEMP II Laboratory Devices apparatus. UV-Visible spectra were recorded on a HP 8453 spectrophotometer in THF and MeOH or on a Shimadzu UV-1800. Emission spectra were recorded on Edinburgh Instruments FS920 spectrofluorometer. Quantum yields were calculated as

reported by equation 1.[38] ESI-MS measurements were carried out on a Thermo Fisher Scientific Q Exactive Plus MS. Single crystal suitable for structure analysis were selected from the bulk and mounted on a MiTeGen mounts. Data were collected on a Bruker-Nonius X8 Kappa Apex II diffractometer by ω and φ scans using MoKα radiation (λ = 0.71073 Å). Corrections for Lorentz and polarization effects, and absorption were made using SADABS.[39] All five structures were solved using direct methods and refined using full-matrix least squares (on F^2) using the SHELX software package.[40] All non-hydrogen atoms were refined anisotropically. Unless otherwise mentioned, H atoms were added at calculated positions, with coordinates and U_{iso} values allowed to ride on the parent atom. When H atoms participate in hydrogen bonding, their coordinates, but not U_{iso}, are allowed to refine for calculation of hydrogen bond analysis. Cyclic voltammetry (CV) experiments were carried out on a BASi CV-50W Potentiostat using a platinum working electrode (diameter 1.6 mm), a platinum wire as an auxiliary electrode, and a silver wire (diameter 1.0 mm) as a pseudo-reference electrode. The compounds were dissolved in 0.1 M n-Bu_4PF_6 as the supporting electrolyte in dried and degassed THF. Fc/Fc^+ was used as an internal standard (-4.8 eV vs NHE). A scan rate of 50 mV/s was employed. The Pt working electrode required cleaning between samples. The LUMO energies were determined from the onsets of the first reduction waves.

Syntheses.

General Procedure for Buchwald-Hartwig amination (GP1). BrettPhos Pd G1, Methyl *t*-Butyl Ether Adduct (2 mol%)[21], cesium carbonate (2 eq.), dry *t*-butanol (2 mL), **1** (1 eq.), and aniline (2 eq.) were added to a scintillation vial equipped with a cross stir bar in a dry box. The reaction mixture was stirred at 80 °C and monitored by TLC for completion.

General Procedure for acid-mediated cyclization (GP2). The diazapentacene precursor (2 mmol) was added to a scintillation vial with a cross stir bar and trifluoromethanesulfonic acid (TFMSA) (2 mL) or trifluoroacetic acid (TFA) (2 mL) and TFMSA (400 µL). The reaction was stirred at 60 °C for 1 h. Upon completion, the reaction was cooled and diluted with water. The solution was quenched by adding it to a beaker with 10% NaOH (making sure that the pH of the solution remained basic by pH paper). The precipitate was filtered and rinsed with DI water until the filtrate was not basic.

2,5-Dibromoterephthalonitrile (**1**).[19]

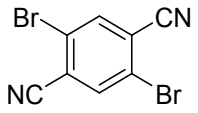

1

2,5-Dibromoterephthaloyl dichloride. 2,5-Dibromoterephthalic acid (11.4 g, 35.0 mmol) was treated with oxalyl chloride (10 mL, 118 mmol) and distilled DMF (10 drops) in DCM (60 mL) and refluxed under N_2 for 3 h. The solvent was removed under reduced pressure and further dried under vacuum to yield a pale-yellow solid (12.6 g, quant.). *2,5-Dibromoterephthalamide.* 2,5-Dibromoterephthaloyl dichloride (12.6 g, 35.0 mmol) was slowly added to a beaker with ammonium hydroxide (50 mL) and stirred at room temperature for 5 min. The precipitate was filtered and rinsed with DI water (60 mL) three times followed by cold acetone (50 mL) to yield a white solid (10.6 g, 94%). **^{1}H NMR** (400 MHz, DMSO-d_6): δ [ppm] = 7.99 (s, 2H); 7.72 (s, 2H); 7.64 (s, 2H). *2,5-Dibromoterephthalonitrile.* 2,5-Dibromoterephthalamide (10.6 g, 33.0 mmol) was added to a round bottom flask followed by phosphoryl chloride (40 mL) and stirred at 110 °C under N_2 for 1 h. It was quenched by slowly adding the reaction mixture to ice water. The precipitate was filtered and rinsed with DI water to afford the pure 2,5-dibromoterephthalonitrile as a colorless solid (8.28 g, 87.8%). **^{1}H NMR** (400 MHz, DMSO-d_6): δ [ppm] = 8.60 (s, 2H); **^{13}C{H} NMR** (100 MHz, DMSO-d_6): δ [ppm] = 115.3, 120.1, 124.1, 138.3; **IR** (neat): 1/λ [cm^{-1}] = 3078, 3010, 2233, 1811; **R_f** (SiO_2, 80:20 (hexanes:ethyl acetate)): 0.35; **m.p.**: 269-272 °C.

2,5-bis(phenylamino)terephthalonitrile (**2a**).

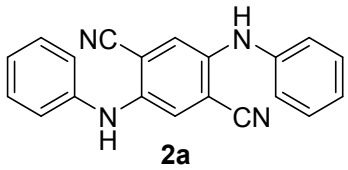

2a

2a was prepared via procedure **GP1** using Brettphos Pd G1 (317 mg, 40.0 µmol), cesium carbonate (1.33 g, 4.09 mmol), *t*-butanol (4 mL), **1** (576 mg, 2.01 mmol), and aniline (380 µL, 4.16 mmol). After 2 h., the reaction was cooled, and the solvent was removed under vacuum. Once dried, acetone (2 mL) was added to the vial and the contents were filtered over Celite. The solid was rinsed with acetone (3x with 2 mL) and the filtrate collected in an Erlenmeyer flask was discarded. In a clean Erlenmeyer flask, the solid was rinsed with 1,4-dioxane (~125 mL) until the filtrate was no longer fluorescent. The filtrate was reduced under vacuum and the solid was rinsed with acetone (2x with 1 mL) and dried under vacuum to give an orange solid (587 mg, 93.9%). **^{1}H NMR** (400 MHz,

DMSO-d_6): δ [ppm] = 6.92-6.95 (t, J = 7.4 Hz, 2H), 7.05-7.07 (d, J = 7.8 Hz, 4H), 7.26-7.30 (t, J = 7.8 Hz, 4H), 7.55 (s, 2H), 8.43 (s, 2H); **^{13}C{H} NMR** (100 MHz, DMSO-d_6): δ [ppm] = 108.6, 116.4, 117.7, 121.3, 124.7, 129.4, 139.8, 142.8; **IR** (neat): 1/λ [cm^{-1}] = 3588, 3482, 3323, 3060, 2215, 1660, 1601, 1579, 1524; **λ_{max}** (THF): 438 nm; HRMS (ESI-orbitrap) *m/z* **[M+H]$^+$**: calcd for $C_{20}H_{15}N_4$: 311.1291, found: 311.1298; **R_f** (SiO_2, 80:20 (hexanes:ethyl acetate)): 0.26.

quinolino[2,3-b]acridine-7,14-diamine (**2b**).

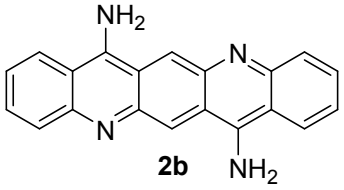

2b was prepared via procedure **GP2** using **2a** (633 mg, 2.04 mmol) and TFMSA (2.00 mL, 22.6 mmol). After rinsing with DI water, the solid was rinsed with ethyl acetate until the filtrate was colorless. The solid was dried in an oven for 15 h. at 105 °C to yield a purple product (600 mg, 94.8%). **^{1}H NMR** (400 MHz, DMSO-d_6): δ [ppm] = 7.22-7.26 (t, J = 7.5 Hz, 2H), 7.62-7.66 (t, J = 7.5 Hz, 2H), 7.71-7.73 (d, J = 9.2 Hz, 2H), 8.38-8.40 (d, J = 8.3 Hz, 2H), 8.94 (s, 2H); **^{13}C{H} NMR** (100 MHz, DMSO-d_6): δ [ppm] = 112.1, 118.7, 119.2, 121.7, 124.6, 125.3, 132.1, 140.2, 146.8, 153.6; **λ_{max}** (THF): 648 nm; HRMS (ESI-orbitrap) *m/z* **[M+H]$^+$**: calcd for $C_{20}H_{15}N_4$: 311.1291, found: 311.1290.

2,5-bis((4-hexylphenyl)amino)terephthalonitrile (**3a**).

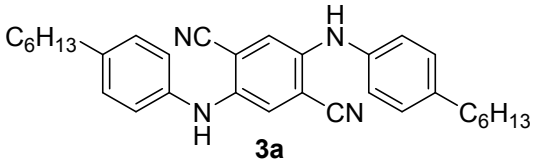

3a was prepared via procedure **GP1** using Brettphos Pd G1 (354 mg, 44.3 μmol), cesium carbonate (1.47 g, 4.50 mmol), *t*-butanol (4 mL), **1** (572 mg, 2.00 mmol), and 4-hexylaniline (800 μL, 4.15 mmol). After 2 h., the reaction was cooled and diluted with methanol (5 mL) and filtered over Celite. The solid was rinsed with methanol (10 mL) followed by acetone (2 mL) and the filtrate collected in an Erlenmeyer flask was discarded. In a clean Erlenmeyer flask, the solid was rinsed with chloroform (~150 mL) until the filtrate was no longer fluorescent. The filtrate was reduced under vacuum and the crude product was sublimed at 110 °C to remove the dihalide starting material to yield the product as a bright, orange solid (741 mg, 77.4%). **^{1}H NMR** (400 MHz, $CDCl_3$-*d*): δ [ppm] = 0.90-0.93 (t, 6H), 1.34-1.40 (m, 12H), 1.60-1.67 (q, 4H), 2.60-2.63 (t, 4H), 6.00 (s, 2H), 7.02-7.05 (d, J = 8.3 Hz, 4H), 7.19-7.21 (d, J = 8.3 Hz, 4H), 7.30 (s, 2H); **^{13}C{H} NMR** (100 MHz, $CDCl_3$-*d*): δ [ppm] = 14.1, 22.6, 29.0, 31.5, 31.7, 35.3, 104.6, 116.2, 118.9, 121.3, 129.7, 137.5, 139.3, 139.8; **IR** (neat): 1/λ [cm^{-1}] = 3319, 2958, 2919, 2852, 2219, 1613, 1589, 1532; **λ_{max}** (THF): 445 nm; HRMS (ESI-orbitrap) *m/z* **[M+H]$^+$**: calcd for $C_{32}H_{39}N_4$: 479.3169, found: 479.3166; **R_f** (SiO_2, 80:20 (hexanes:ethyl acetate)): 0.48.

2,9-dihexylquinolino[2,3-b]acridine-7,14-diamine (**3b**).

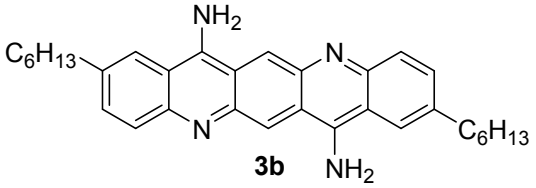

3b was prepared via procedure **GP2** using **3a** (943 mg, 1.97 mmol) and TFMSA (2.00 mL, 22.6 mmol). After rinsing with DI water, the solid was rinsed with dichloromethane until the filtrate was colorless. The solid was dried in an oven for 15 h. at 105 °C to yield

a purple product (936 mg, 99.2%). **^{1}H NMR** (700 MHz, cryoprobe, DMSO-d_6): δ [ppm] = 0.88-0.90 (t, 6H), 1.31-1.38 (m, 12H), 1.71-1.75 (q, 4H), 2.80-2.820 (t, 4H), 7.93-7.94 (d, J = 7 Hz, 2H), 7.96-7.97 (d, J = 7 Hz, 2H), 8.47 (s, 2H), 8.97 (s, 2H); **^{13}C{H} NMR** (176 MHz, cryoprobe, DMSO-d_6): δ [ppm] = 14.4, 22.5, 28.8, 31.0, 31.6, 35.4, 111.0, 114.9, 118.1, 119.4, 120.2, 122.0, 123.3, 133.7, 138.9, 140.2, 158.5; **λ_{max}** (THF): 649 nm; HRMS (ESI-orbitrap) *m/z* **[M+H]$^+$**: calcd for $C_{32}H_{39}N_4$: 479.3169, found: 479.3155.

2,5-bis((4-(tert-butyl)phenyl)amino)terephthalonitrile (**4a**).

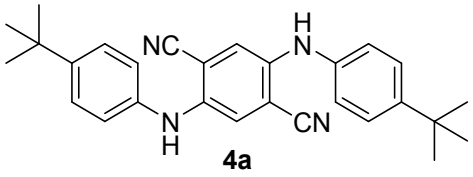

4a

4a was prepared via procedure **GP1** using Brettphos Pd G1 (490 mg, 61.3 μmol), cesium carbonate (1.99 g, 6.14 mmol), *t*-butanol (6 mL), **1** (903 mg, 3.16 mmol), and 4-*t*-butylaniline (1.00 mL, 6.28 mmol). After 2 h., the reaction was cooled and diluted with methanol (5 mL) and filtered over Celite. The solid was rinsed with methanol (15 mL) followed by acetone (2 mL) and the filtrate collected in an Erlenmeyer flask was discarded. In a clean Erlenmeyer flask, the solid was rinsed with chloroform (~200 mL) until the filtrate was no longer fluorescent. The filtrate was reduced under vacuum to yield the product as a yellow solid (1.20 g, 90.4%). **^{1}H NMR** (400 MHz, $CDCl_3$-*d*): δ [ppm] = 1.36 (s, 18H), 6.02 (s, 2H), 7.05-7.07 (d, J = 8.8 Hz, 4H), 7.34 (s, 2H), 7.40-7.42 (d, J = 8.8 Hz, 4H); **^{13}C{H} NMR** (100 MHz, $CDCl_3$-*d*): δ [ppm] = 31.4, 34.4, 104.7, 116.2, 119.0, 120.8, 126.7, 137.3, 139.7, 147.4; **IR** (neat): 1/λ [cm^{-1}] = 3328, 2947, 2898, 2863, 2237, 2217, 1613, 1593, 1536; **λ_{max}** (THF): 448 nm; HRMS (ESI-orbitrap) *m/z* **[M+H]$^+$**: calcd for $C_{28}H_{31}N_4$: 423.2543, found: 423.2535; **R_f** (SiO_2, 80:20 (hexanes:ethyl acetate)): 0.24.

2,9-di-tert-butylquinolino[2,3-b]acridine-7,14-diamine (**4b**).

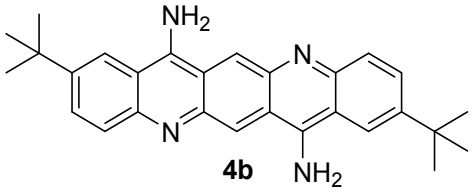

4b

4b was prepared via procedure **GP2** using **4a** (856 mg, 2.02 mmol), TFA (2 mL, 26.1 mmol) and TFMSA (400 μL, 4.52 mmol). After rinsing with DI water, the solid was rinsed with chloroform until the filtrate was colorless. The solid was dried in an oven for 15 h. at 105 °C to yield a purple product (665 mg, 77.7%). **^{1}H NMR** (700 MHz, cryoprobe, DMSO-d_6): δ [ppm] = 1.42 (s, 18H), 7.71-7.72 (d, J = 7 Hz, 2H), 7.80-7.81 (d, J = 7 Hz, 2H), 8.26 (s, 2H), 9.00 (s, 2H); **^{13}C{H} NMR** (176 MHz, cryoprobe, DMSO-d_6): δ [ppm] = 31.5, 35.4, 111.0, 118.9, 125.7, 131.2, 140.3, 144.2, 146.0, 152.9; **λ_{max}** (THF): 595 nm; HRMS (ESI-orbitrap) *m/z* **[M+H]$^+$**: calcd for $C_{28}H_{31}N_4$: 423.2543, found: 423.2524.

ASSOCIATED CONTENT

Supporting Information. ^{1}H and ^{13}C NMR, UV-visible spectroscopy, mass spectrometry, and X-ray crystallography.

AUTHOR INFORMATION

Corresponding Author

*cbgorman@ncsu.edu

ACKNOWLEDGMENT

The authors would like to acknowledge the financial support by ACS Petroleum Research Fund (Grant PRF# 57251-ND7). We also thank Prof. F. N. Castellano and Chris Papa for helpful discussions and assistance with photophysical measurements. All nuclear magnetic resonance, mass spectrometry, and X-ray crystallography measurements were made in the Molecular Education, Technology, and Research Innovation Center (METRIC) at NC State University.

REFERENCES

(1) Guo, X.; Xu, Y.; Ogier, S.; Ng, T. N.; Caironi, M.; Perinot, A.; Li, L.; Zhao, J.; Tang, W.; Sporea, R. A.; et al. Current Status and Opportunities of Organic Thin-Film Transistor Technologies. *IEEE Trans. Electron Devices* **2017**, *64* (5), 1906–1921.

(2) Usta, H.; Facchetti, A.; Marks, T. J. N -Channel Semiconductor Materials Design for Organic Complementary Circuits. *Acc. Chem. Res.* **2011**, *44* (7), 501–510.

(3) Naibi Lakshminarayana, A.; Ong, A.; Chi, C. Modification of Acenes for N-Channel OFET Materials. *J. Mater. Chem. C* **2018**, *6* (14), 3551–3563.

(4) Wang, C.; Dong, H.; Hu, W.; Liu, Y.; Zhu, D. Semiconducting π-Conjugated Systems in Field-Effect Transistors: A Material Odyssey of Organic Electronics. *Chem. Rev.* **2012**, *112* (4), 2208–2267.

(5) Quinn, J. T. E.; Zhu, J.; Li, X.; Wang, J.; Li, Y. Recent Progress in the Development of N-Type Organic Semiconductors for Organic Field Effect Transistors. *J. Mater. Chem. C* **2017**, *5* (34), 8654–8681.

(6) Zhao, Y.; Guo, Y.; Liu, Y. 25th Anniversary Article: Recent Advances in n-Type and Ambipolar Organic Field-Effect Transistors. *Adv. Mater.* **2013**, *25* (38), 5372–5391.

(7) Anthony, J. E. Functionalized Acenes and Heteroacenes for Organic Electronics. *Chem. Rev.* **2006**, *106* (12), 5028–5048.

(8) Zhao, Y.; Mondal, R.; Neckers, D. C. Photochemical Formation of Substituted Pentacenes. *J. Org. Chem.* **2008**, *73* (14), 5506–5513.

(9) Liang, Z.; Tang, Q.; Xu, J.; Miao, Q. Soluble and Stable N-Heteropentacenes with High Field-Effect Mobility. *Adv. Mater.* **2011**, *23* (13), 1535–1539.

(10) Shi, X.; Chi, C. Different Strategies for the Stabilization of Acenes and Acene Analogues. *Chem. Rec.* **2016**, *16* (3), 1690–1700.

(11) Bunz, U. H. F. The Larger N-Heteroacenes. *Pure Appl. Chem.* **2010**, *82* (4), 953–968.

(12) Bunz, U. H. F.; Engelhart, J. U.; Lindner, B. D.; Schaffroth, M. Large N-Heteroacenes: New Tricks for Very Old Dogs? *Angew. Chemie - Int. Ed.* **2013**, *52* (14), 3810–3821.

(13) Bunz, U. H. F.; Freudenberg, J. N-Heteroacenes and N-Heteroarenes as N-Nanocarbon Segments. *Acc. Chem. Res.* **2019**, *52*, 1575–1587.

(14) Isoda, K. Acid-Responsive N -Heteroacene-Based Material Showing Multi-Emission Colors. *ChemistryOpen* **2017**, *6* (2), 242–246.

(15) Bunz, U. H. F. The Larger Linear N-Heteroacenes. *Acc. Chem. Res.* **2015**, *48* (6), 1676–1686.

(16) Lunchev, A. V; Hendrata, V. C.; Jaggi, A.; Morris, S. A.; Ganguly, R.; Chen, X.; Sun, H.; Grimsdale, A. C. A Friedländer Route to 5,7-Diazapentacenes. *J. Mater. Chem. C* **2018**, *6* (14), 3715–3721.

(17) Bunz, U. H. F.; Engelhart, J. U. The Palladium Way to N-Heteroacenes. *Chem. - A Eur. J.* **2016**, *22* (14), 4680–4689.

(18) Lunchev, A.; Morris, S.; Ganguly, R.; Grimsdale, A. C. Synthesis and Electronic Properties of Novel 5,7-Diazapentacene Derivatives. *Chem. - A Eur. J.* **2018**, *25* (7), 1819–1823.

(19) Cheng, J. Z.; Lin, C. C.; Chou, P. T.; Chaskar, A.; Wong, K. T. Fluorene as the π-Spacer for New Two-Photon Absorption Chromophores. *Tetrahedron* **2011**, *67* (4), 734–739.

(20) Surry, D. S.; Buchwald, S. L. Dialkylbiaryl Phosphines in Pd-Catalyzed Amination: A User's Guide. *Chem. Sci.* **2011**, *2* (1), 27–50.

(21) Fors, B. P.; Watson, D. A.; Biscoe, M. R.; Buchwald, S. L. A Highly Active Catalyst for Pd-Catalyzed Amination Reactions: Cross-Coupling Reactions Using Aryl Mesylates and the Highly Selective Monoarylation of Primary Amines Using Aryl Chlorides. *J. Am. Chem. Soc.* **2008**, *130* (41), 13552–13554.

(22) Fraleoni-morgera, A.; Zanirato, P. BF3.OEt2-Promoted Synthesis of Acridines via N-Aryl Nitrenium-BF3 Ions Generated by Dissociation of 2-Oxo Azidoarenes in Benzene. *Arkivoc* **2006**, *2006* (12), 111–120.

(23) Solà, M. Forty Years of Clar's Aromatic π-Sextet Rule. *Front. Chem.* **2013**, *1* (22), 1–8.

(24) Kuninobu, Y.; Tatsuzaki, T.; Matsuki, T.; Takai, K. Indium-Catalyzed Construction of Polycyclic Aromatic Hydrocarbon Skeletons via Dehydration. *J. Org. Chem.* **2011**, *76* (17), 7005–7009.

(25) Anthony, J. E. The Larger Acenes: Versatile Organic Semiconductors. *Angew. Chemie - Int. Ed.* **2008**, *47* (3), 452–483.

(26) Zhou, K.; Dong, H.; Zhang, H.-L.; Hu, W. High Performance N-Type and Ambipolar Small Organic Semiconductors for Organic Thin Film Transistors. *Phys. Chem. Chem. Phys.* **2014**, *16* (41), 22448–22457.

(27) Gafni, A.; Brand, L. Excited State Proton Transfer Reactions of Acridine Studied by Nanosecond Fluorometry. *Chem. Phys. Lett.* **1978**, *58* (3), 346–350.

(28) Müller, M.; Reiss, H.; Tverskoy, O.; Rominger, F.; Freudenberg, J.; Bunz, U. H. F. Stabilization by Benzannulation: Butterfly Azaacenes. *Chem. - A Eur. J.* **2018**, *24* (49), 12801–12805.

(29) Gómez, P.; Georgakopoulos, S.; Cerón, J. P.; da Silva, I.; Más-Montoya, M.; Pérez, J.; Tárraga, A.; Curiel, D. Hydrogen-Bonded Azaphenacene: A Strategy for the Organization of π-Conjugated Materials. *J. Mater. Chem. C* **2018**, *6* (15), 3968–3975.

(30) Talacki, R.; Carrell, H. L.; Glusker, J. P. 9-Aminoacridine Hydrochloride Monohydrate. *Acta Crystallogr. Sect. B Struct. Crystallogr. Cryst. Chem.* **1974**, *30* (4), 1044–1047.

(31) Fossey, J.; Loupy, A.; Strzelecka, H. An Ab Initio Study of Protonation and Alkylation of Aminopyridine. *Tetrahedron* **1981**, *37* (10), 1935–1941.

(32) Liang, Z.; Tang, Q.; Mao, R.; Liu, D.; Xu, J.; Miao, Q. The Position of Nitrogen in N-Heteropentacenes Matters. *Adv. Mater.* **2011**, *23* (46), 5514–5518.

(33) Rüdiger, E. C.; Müller, M.; Koser, S.; Rominger, F.; Freudenberg, J.; Bunz, U. H. F. Dibenzohexacene: Stabilization Through Additional Clar Sextets. *Chem. - A Eur. J.* **2018**, *24* (5), 1036–1040.

(34) Kaur, I.; Jia, W.; Kopreski, R. P.; Selvarasah, S.; Dokmeci, M. R.; Pramanik, C.; McGruer, N. E.; Miller, G. P. Substituent Effects in Pentacenes: Gaining Control over HOMO−LUMO Gaps and Photooxidative Resistances. *J. Am. Chem. Soc.* **2008**, *130* (48), 16274–16286.

(35) Liu, K.; Song, C.; Zhou, Y.; Zhou, X.; Pan, X.; Cao, L.; Zhang, C.; Liu, Y.; Gong, X.; Zhang, H. Tuning the Ambipolar Charge Transport Properties of N-Heteropentacenes by Their Frontier Molecular Orbital Energy Levels †. *J. Mater. Chem. C* **2015**, *3*, 4188–4196.

(36) Maliakal, A.; Raghavachari, K.; Katz, H.; Chandross, E.; Siegrist, T. Photochemical Stability of Pentacene and a Substituted Pentacene in Solution and in Thin Films. *Chem. Mater.* **2004**, *16* (24), 4980–4986.

(37) Zade, S. S.; Bendikov, M. Reactivity of Acenes: Mechanisms and Dependence on Acene Length. *J. Phys. Org. Chem.* **2012**, *25* (6), 452–461.

(38) Brouwer, A. M. Standards for Photoluminescence Quantum Yield Measurements in Solution (IUPAC Technical Report). *Pure Appl. Chem.* **2011**, *83* (12), 2213–2228.

(39) G. M. Sheldrick. Crystal Structure Refinement with SHELXL. *Acta Crystallogr. Sect. C Struct. Chem.* **2015**, *C71*, 3–8.

(40) Sheldrick, G. M. A Short History of SHELX. *Acta Crystallogr. Sect. A Found. Crystallogr.* **2008**, *64* (1), 112–122.

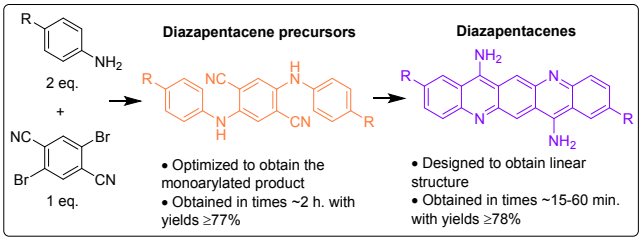
Diazapentacene precursors
Diazapentacenes
2 eq.
1 eq.
• Optimized to obtain the monoarylated product
• Obtained in times ~2 h. with yields ≥77%
• Designed to obtain linear structure
• Obtained in times ~15-60 min. with yields ≥78%